



Title	Integrated Multilayer Flow System on a Microchip.
Author(s)	HIBARA, Akihide; TOKESHI, Manabu; UCHIYAMA, Kenji; HISAMOTO, Hideaki; KITAMORI, Takehiko
Citation	Analytical Sciences, 17(1), 89-93 https://doi.org/10.2116/analsci.17.89
Issue Date	2001-01
Doc URL	http://hdl.handle.net/2115/71674
Type	article
File Information	Anal.sci.17-89.pdf



[Instructions for use](#)

Integrated Multilayer Flow System on a Microchip

Akihide HIBARA,^{*†} Manabu TOKESHI,^{**} Kenji UCHIYAMA,^{**} Hideaki HISAMOTO,^{*}
and Takehiko KITAMORI^{*,**,***}

^{*}*Department of Applied Chemistry, School of Engineering, The University of Tokyo,
Hongo, Bunkyo, Tokyo 113-8656, Japan*

^{**}*Integrated Chemistry Project, Kanagawa Academy of Science and Technology,
Sakado, Takatsu, Kawasaki 213-0012, Japan*

^{***}*Precursory Research for Embryonic Science and Technology 21,
Japan Science and Technology Corporation*

We utilized microchip technology and found that the multilayer flow of liquids can be formed in microchannels. Liquid/liquid interfaces were formed parallel to the side wall of the microchannels, because the surface tension and friction force are stronger than the force of gravity. A water/ethylacetate/water interface was formed in a 70- μm -wide and 30- μm -deep channel. The interface was observed to be quite stable and to be maintained for a distance of more than 18 cm. As an example of a multilayer flow application, we demonstrated the liquid/liquid extraction of Co-dimethylaminophenol complex in a microchannel. The solvent-extraction process of the complex into *m*-xylene in the multilayer flow was found to reach equilibrium in 4 s, while it took 60 s in a simple two-phase extraction.

(Received September 26, 2000; Accepted October 16, 2000)

Introduction

Microchip technology has become of major interest to analytical chemists lately due to its desirable characteristics, such as reductions in consumed reagents, space requirements, and necessary analytical times. Micro systems utilizing microchips are well known as micro total analysis systems, labs-on-a-chip or integrated chemistry labs.^{1,2} In our previous papers, we demonstrated the advantages of microchips in many applications, including flow-injection analysis,^{3,4} solvent extraction,^{5,6} immunoassay,⁷ organic synthesis⁸ and laser reaction control.⁹ The microchannels in the microchips were characterized by small volume, short diffusion length, large specific interface (solid/liquid or liquid/liquid), and small heat capacity. By utilizing these characteristics, micro chemical systems are expected to offer improved performances over conventional systems.

In microchip technology, separation and molecular transport is doubtlessly one of the key processes. Since the flow in a microchannel is a distinctive feature of the microchip, and the flow can be easily controlled to make contact with other flows, a molecular transport control technique from one flow to another is quite important.

From the viewpoint of inter-flow molecular transport, Yager's group proposed a T-sensor and H-filter system.^{10,11} The H-filter system consists of sample and receptor aqueous flows. In the system, only a small species in the sample flow is transported to receptor flow due to the large diffusivity of the small species. Although the H-filter system is effective for separation based on a diffusivity difference, another technique based on chemical

properties is required for general applications of microchips. In Refs. 5 and 6, we proposed a new technique, *i.e.*, a solvent-extraction system on a microchip. In the extraction system, a liquid/liquid interface is formed along the microchannel, where aqueous and organic solutions are introduced with different flows and the subject substance is transported through the interface. Since this transport is based on the distribution ratio of the substance, we can control the transport by selecting the compositions of the solutions.

One distinct feature of our system is parallel liquid/liquid interfaces to the side wall. This feature has also been reported by Kim *et al.*¹² Our main idea of the present article is to utilize this feature so that multilayer flow having liquid/liquid interfaces can be formed in a microchip. Multilayer flow is expected to drastically improve experimental techniques in various fields. In particular, it should have a great impact on liquid membrane transport experiments.¹³ Usually, liquid membrane transport uses a large-sized U-shaped tube to form more than two interfaces, or it uses a polymer membrane to support the organic phase. In the conventional methods, the effects of high-speed stirring, which is required to enhance the transport, and of polymer matrix should be considered. If our idea of multilayer flow is realized, the transport through a thin native liquid membrane of 10- μm order can be investigated. In this case, analysis becomes very simple because we consider only diffusion and interphase transport.

In this study, we demonstrated that quite stable multilayer flow can be formed in a microchannel. At first, we discussed why a parallel interface can be formed in the microchannel. We focused scaling effects on the relationship between gravity and interfacial tension. Next, a microchip with a three-layer flow microchannel pattern was fabricated by using a photolithographic wet etching method. We observed miscible and immiscible multilayer flows in the microchip, that is,

[†] To whom correspondence should be addressed.

E-mail: hibara@icl.t.u-tokyo.ac.jp

water/acetone/water and water/ethylacetate/water flows. We also demonstrated solvent extraction in a water/*m*-xylene/water multilayer flow. Co-dimethylaminophenol complex was dissolved in both aqueous phases and *m*-xylene was used as an extraction phase. The extraction process was compared with that for a simple two-layer flow. Finally, we proposed some future applications of the multilayer flow system.

Experimental

Microchip fabrication and operation

Microchips were fabricated by using a photolithographic wet etching method. A mechanically polished 0.7-mm-thick pyrex glass plate was the substrate (bottom plate). The substrate plates were annealed at 570°C for 5 h before use. For good contact between the substrates and the photoresist and protection of the substrates during glass etching, 20-nm-thick Cr and 100-nm-thick Au layers were evaporatively deposited on the substrates under a vacuum. A 2- μm -thick positive photoresist was spin-coated on the metal and baked at 90°C for 30 min. UV light was exposed through a photomask by using a mask aligner to transfer the microchannel pattern onto the photoresist. The photoresist was developed and a pattern with 10- μm -wide lines was obtained. The Au and Cr layers were etched with $\text{I}_2/\text{NH}_4\text{I}$ and $\text{Ce}(\text{NH}_4)_2(\text{NO}_3)_6$ solutions. The bare glass surface with the microchannel pattern was etched with a 50% HF solution at an etching rate of 13 $\mu\text{m}/\text{min}$. After glass etching, the remaining photoresist was removed in acetone and metals were removed in $\text{I}_2/\text{NH}_4\text{I}$ and $\text{Ce}(\text{NH}_4)_2(\text{NO}_3)_6$ solutions. Inlet and outlet holes were drilled by ultrasonic sandblasting on another pyrex glass substrate (cover plate). The cover and etched plates were thermally laminated in a furnace at 650°C for 5 h after washing in an ethanol and NaOH solution.

The operation procedures have been presented elsewhere.⁵ Briefly, the flow rates of the liquid samples were controlled by syringes and microsyringe pumps. Each syringe needle was connected to a Teflon screw with an o-ring and a fused-silica capillary tube using epoxy glue. Teflon screws were set on PVC holders which sandwiched the microchip.

Apparatus

Liquid flows in the microchannel were observed by a biological microscope with an objective lens ($\times 20$, N. A. 0.46). The images of the flows were obtained by a CCD camera.

We have already made a detailed description of the thermal lens microscope.^{14,15} In summary, a 488-nm emission line of an argon ion laser and a 633-nm emission line of a helium-neon laser were used as excitation and probe beams. The excitation beam was modulated at 1 kHz by an optical chopper. After the beam diameters were expanded, the excitation and probe beams were made coaxial by a dichroic mirror just before they were introduced into an objective lens whose magnification and numerical aperture were 20-fold and 0.46, respectively. The beam waist and confocal length of the excitation beam were 1.3 μm and 10.8 μm , respectively. Samples were set in the center of the confocal volume of the excitation beam. Due to the spatial profile of the laser intensity and thermal diffusion after light absorption, intermittent irradiation of the excitation beam produced a repeated spatial temperature profile in/around the waist. Since the reflective index of solvents depends on the temperature, the temperature profile acted as a transient lens. In order to optimize the thermal lens setup, the focal point of the probe beam was set 10 μm lower than that of the excitation beam by controlling the divergence of the probe beam. The

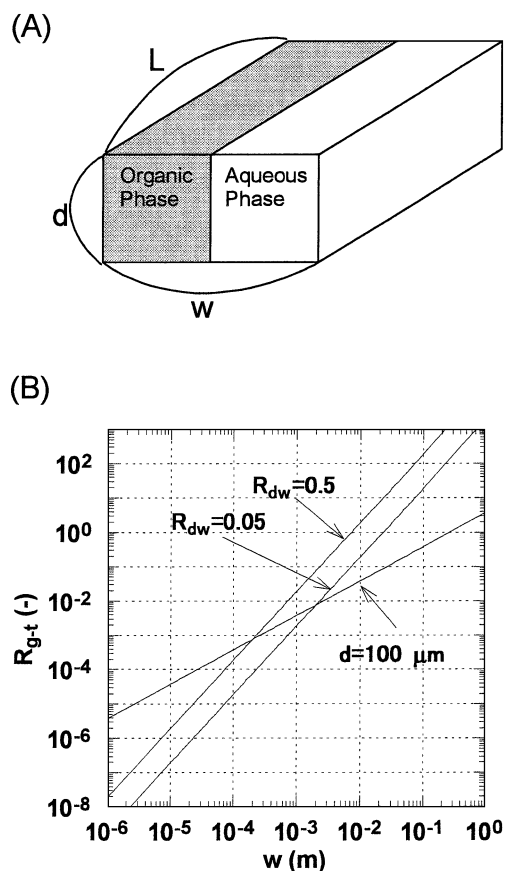


Fig. 1 (A) Illustration of a model liquid/liquid interface between organic solvent and water. The depth-to-width aspect ratio, R_{dw} , is defined as d/w . (B) Dependences of the dimensionless number R_{g-t} on the microchannel width.

focal point of the probe beam was shifted by the temporal lens and, therefore, the probe-beam intensity after passing through a counter objective lens, an interference filter and a pinhole was modulated at the same frequency as an optical chopper. The probe intensity was detected by a photodiode and the output current was fed into a lock-in amplifier. The synchronous signal with the chopper was recorded as a thermal lens signal.

Results and Discussion

Scaling

To clarify the features of the liquid/liquid interfaces in the microchannel, the size dependence of the interfacial parameters was analyzed by a dimensionless analysis. We analyzed a model microchannel having a square cross section. The model microchannel is illustrated in Fig. 1(A). The depth, width and length along the microchannel are represented as d , w and L , respectively. As a normal indicator of the microchannel, a depth-to-width aspect ratio, R_{dw} , is defined as

$$R_{dw} = \frac{d}{w}. \quad (1)$$

When the same volumes of organic and aqueous phases are introduced into the microchannel, the width of each phase becomes $w/2$. The interfacial tension and gravity difference between the two phases are expressed as $2\gamma(d + L)$ and

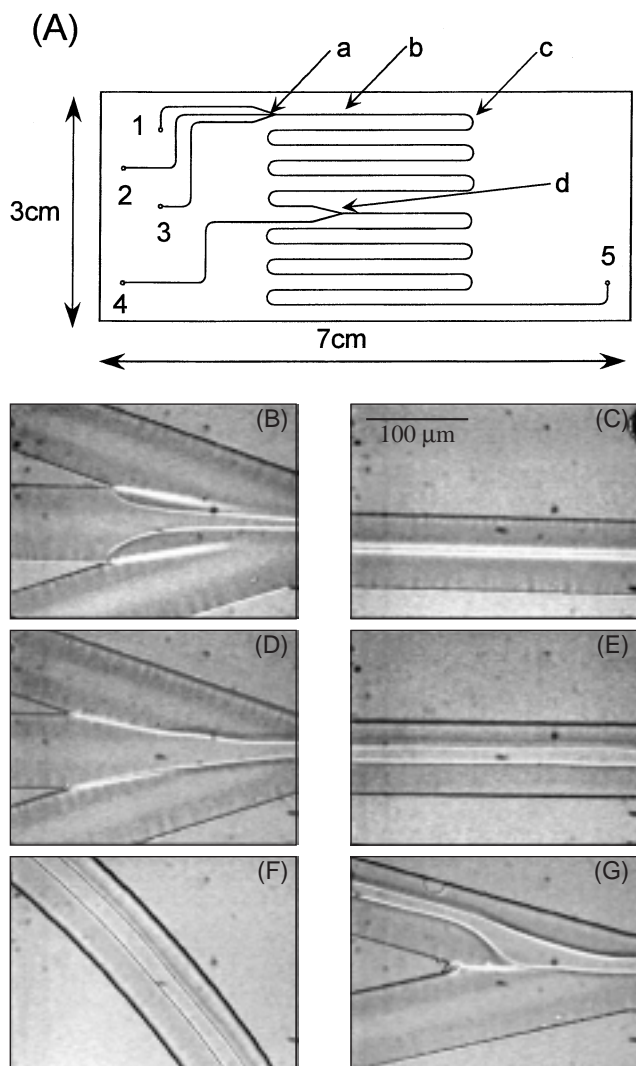


Fig. 2 (A) Microchannel pattern for a multilayer flow system. Inlet flows from 1, 2 and 3 join at the junction (point a) with incident angles of 18° . The folded part (point c) has a curvature radius of 1 mm. Another inlet flow from 4 joins to the main channel with an incident angle of 28° . (B) Water/acetone/water (WAW) flow at the junction (point a). (C) WAW flow 10 mm downstream from the junction (point b). (D) Water/ethylacetate/water (WEW) flow at the junction (point a). (E) WEW flow at downstream (point b). (F) WEW flow at the curved channel (point c). (G) WEW flow at another junction (point d).

$\Delta\rho dwLg/2$, where γ and $\Delta\rho$ are the interfacial energy and the density difference between the two phases and g is the gravitational acceleration ($= 9.8 \text{ m/s}^2$). To compare the contributions of these two forces to the interface, a dimensionless number representing gravity-to-tension ratio, R_{g-t} , is defined as

$$R_{g-t} = \frac{\Delta\rho dwLg/2}{2\gamma(L+d)}. \quad (2)$$

Here, L is assumed to be sufficiently longer than d , because our microchannel is sufficiently longer than its width. By using this assumption, we can simplify Eq. (2) as

$$R_{g-t} = \frac{\Delta\rho dwg}{4\gamma}. \quad (3)$$

By using the aspect ratio presented in Eq. (1), Eq. (3) is formulized as

$$R_{g-t} = R_{dw} \frac{\Delta\rho g}{4\gamma} w^2. \quad (4)$$

The calculation results of R_{g-t} for R_{dw} of 0.5 and 0.05 and a fixed depth of $100 \mu\text{m}$ are plotted in Fig. 1(B). The former two are for a fixed aspect-ratio case (Eq. (4)) and the latter is for a fixed-depth case (Eq. (3)). The cases of $R_{dw} = 0.5$ and $d = 100 \mu\text{m}$ correspond to the microchannel we reported in Refs. 5 and 6. The case of $R_{dw} = 0.05$ corresponds to a flatter microchannel, which was used by Kim *et al.*¹² Since the ethylacetate/water interface is discussed in the following section, the values of $\Delta\rho$ and γ for an ethylacetate/water interface ($\Delta\rho = 0.1075 \times 10^3 \text{ kg/m}^3$ and $\gamma = 6.8 \times 10^{-3} \text{ N/m}$) were used for the calculation. The calculation gives the relationships $R_{g-t} = 1.9 \times 10^4 \times w^2$ ($R_{dw} = 0.5$), $1.9 \times 10^3 \times w^2$ ($R_{dw} = 0.05$) and $3.8 \times w$ ($d = 100 \mu\text{m}$). As shown in Fig. 1(B), R_{g-t} is less than 10^{-3} for $d = 100 \mu\text{m}$ (10^{-4} m), which means the contribution of gravity can be neglected for interfaces in microchannels with $100\text{-}\mu\text{m}$ -order scale. This feature can be extended to other organic solvents because the ethylacetate/water interface has a smaller interfacial energy than almost all other organic solvent/water interfaces. For example, the coefficient of the relation between R_{g-t} and w^2 (for $R_{dw} = 0.5$) is $7.6 \times 10^4 \text{ m}^{-2}$ for chloroform and $4.3 \times 10^3 \text{ m}^{-2}$ for *m*-xylene.

Our dimensionless analysis showed the validity of our qualitative explanation for the side-by-side interfaces in Refs. 5 and 6, and suggested that multilayer flows can be formed without the contribution of gravity. Since we focused on the relationship between gravity and interfacial tension in this analysis, the model can describe static interfaces. However, the analysis model should be extended to dynamic interfaces in order to consider the contributions of viscosity and viscoelasticity.

Multilayer flow system

A microchip with the microchannel pattern shown in Fig. 2(A) was used to form multilayer flow. The channel width and depth were $70 \mu\text{m}$ and $30 \mu\text{m}$, respectively. Since the microchip was fabricated by an isotropic wet etching method, the microchannel has a nearly semicircular cross section. The holes labeled 1 to 4 were used as inlet holes, and hole 5 was the drain. Liquid flows from inlets 1, 2 and 3 joined at point a, and flow from inlet 4 joined at point d. The channel length between points a and d was about 18 cm.

At first, we examined a three-layer flow of miscible liquids, that is, a water/acetone/water (WAW) flow. The WAW flow at the junction (point a) is shown in Fig. 2(B). The flow rates were 5, 3 and $5 \mu\text{l/min}$ for water, acetone and water, respectively. The mean flow velocity between points a and d was 13 cm/s . Since the Reynolds number of the flow, which means an inertia-force-to-viscous-force ratio, is less than 10, the flow can be regarded as a laminar flow. As shown in Fig. 2(B), the WAW interface can be observed as a refractive index difference. Since the water/acetone interface has a negative surface free energy and becomes stable with increasing interfacial area, the two liquids should mix immediately. In practice, the mixing process of water and acetone can be observed 10-mm-downstream from the junction (point b), as shown in Fig. 2(C). The WAW interface, clearly shown in Fig. 2(B), is transient and can be obtained only by using special techniques, such as our microchip technology.

Next, we examined a three-layer flow of immiscible liquids, that is, a water/ethylacetate/water (WEW) flow. The WEW

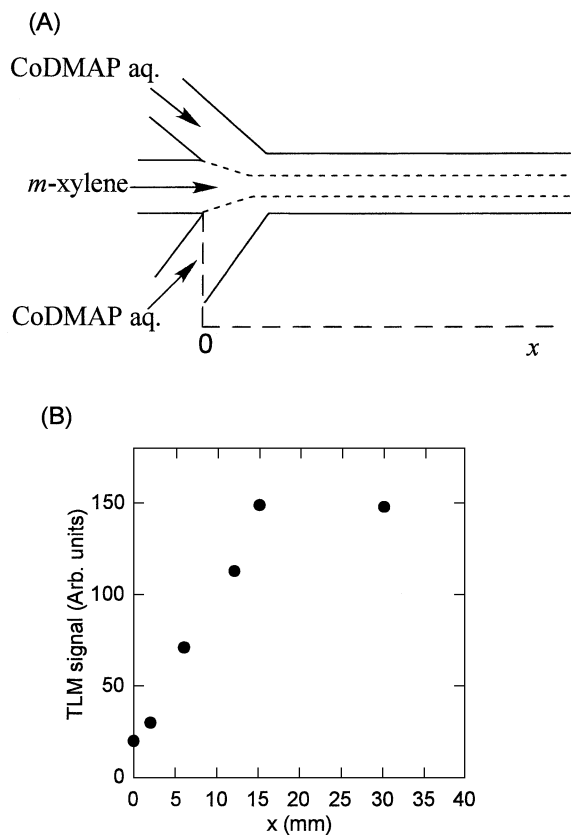


Fig. 3 (A) Schematic illustration of the multilayer extraction system. (B) TLM signal dependence on the distance x .

flows at the junction (point a), 10-mm downstream from the junction (point b), at the curved channel with the curvature radius of 1 mm (point c) and at another water flow junction (point d) are shown in Figs. 2(D) – (G). The thickness of the ethylacetate layer is about 15 μm . The flow rates of water, ethylacetate and water were 3, 5 and 3 $\mu\text{l}/\text{min}$. The mean flow velocity was 11 cm/s. As shown in Figs. 2(D) – (G), the WAW flow maintains the liquid/liquid interfaces for a channel length of more than 18 cm. At the curved channel, the flow is not affected by the inertia force because the effective force in the microchannel is the viscous force and interfacial tension. At the other water flow junction (point d), water flow having a flow rate of 3 $\mu\text{l}/\text{min}$ joins the multilayer flow.

The three-layer flow shown in Figs. 2(D) – (G) realized a very thin (15 μm) liquid membrane which is quite unlike the conventional one. The liquid membrane is expected to drastically improve the experimental methods in various applications. For example, molecular transport through the liquid membrane can be driven only by diffusion due to its quite short diffusion length and time. From the viewpoint of the thin liquid membrane, a centrifugal liquid membrane method has been proposed.¹⁶ Although this centrifugal liquid membrane has a thickness of less than 100 μm , the method can be applied to the liquid/liquid system in order of liquid densities. Since most liquid membrane transport has been studied as a bio-mimetic system, mostly aqueous/organic/aqueous systems have been investigated. In our method utilizing a microchip, the liquid/liquid system with a desirable thickness and desirable order can be formed because our multilayer flow is based on interfacial tension. Under the flow conditions, the time course of the molecular transport is virtually projected to the spatial

distribution of the target molecule along the microchannel. Therefore, molecular distribution measurements across and along the microchannel give time-resolved information. Strictly, the time courses of the transport in static systems differ from those under the two-phase flow condition because the viscosity, viscoelasticity and friction may affect the transport phenomena. Therefore, analysis including these parameters is required.

Solvent extraction in multilayer flow

Recently, we demonstrated a two-layer extraction of Co-dimethylaminophenol (CoDMAP) complex into *m*-xylene in the 250- μm -wide and 100- μm -deep microchannel.⁶ We applied the multilayer system to the solvent extraction of CoDMAP. For the present experiment, a microchip with a 200- μm -wide and 30- μm -deep microchannel was fabricated by the wet-etching method. The *m*-xylene was sandwiched by two aqueous solutions of Co-DMAP (6.5×10^{-6} M) to form a three-layer flow in the microchannel (Fig. 3(A)). The flow rates of aqueous and organic solutions were set as 0.5 $\mu\text{l}/\text{min}$ and 1.0 $\mu\text{l}/\text{min}$. The total flow rate of 2.0 $\mu\text{l}/\text{min}$ corresponded to 0.56 cm/s in the microchannel. The concentration of Co-DMAP in the *m*-xylene phase along the microchannel, which virtually corresponded to the time course of the extraction process, was measured by using a thermal lens microscope (TLM). The dependence of the TLM signal on the distance x from the junction is shown in Fig. 3(B). The extraction process attained equilibrium around a distance of 1.5 cm, which means that the extraction equilibrium was attained within 3 s after contact (three-phase condition, present experiment). In our previous paper,⁶ we reported that the extraction time in a 250- μm -wide microchannel with two-phase stopped flow (two-phase condition, previous experiment) was 60 s.

One explanation for the difference is the diffusion length difference. Since the extraction phase was set at the center, the widths of the extraction and aqueous phases were 67 μm under the three-phase condition, while they were 125 μm under the two-phase condition. The diffusion time, t , for a diffusion length of l is roughly expressed as $t = l^2/D$, where D is the diffusivity. Since the diffusion length under the three-phase condition is about two-times shorter than that under the two-phase condition, the diffusion time is estimated to be four-times shorter.

Another explanation is the large specific interface area (SIA). SIA is defined as an interface-area-to-volume ratio of the extraction phase, and is 300 cm^{-1} under the three-phase condition and 80 cm^{-1} under the two-phase condition. Since a larger SIA corresponds to a larger path of molecules, the large SIA under the three-phase condition may affect the extraction time.

Conclusion

We demonstrated a multilayer flow system integrated on microchips. First, we quantitatively discussed why the parallel interface can be formed in the microchannel. Our analysis showed that interfacial tension had a much larger effect on the interface in the microchannel than gravity. Next, we showed multilayer flow of miscible liquids, the water/acetone/water system, and immiscible liquids, the water/ethylacetate/water system. The immiscible system maintained the liquid/liquid interfaces for a long distance of more than 18 cm. Finally, we demonstrated the solvent extraction of Co-DMAP as a typical application of multilayer flow. We plan to apply the multilayer

flow system to various fields of chemistry, such as liquid membrane transport, non-linear chemical reactions and transport systems, bio-separations utilizing an aqueous two-phase interface, electrochemistry and photo-electrochemistry of a liquid/liquid interface and interfacial synthetic reactions and polymerizations.

Acknowledgements

This research was partially supported by the Shiseido Fund for Science and Technology and Grant-in-Aid for Scientific Research in Priority Area of Electrochemistry of Ordered Interfaces (No. 11118219), for Scientific Research (No. 12042218) and for University and Social Collaboration (No. 11974006) from the Ministry of Education, Science, Sports and Culture of Japan.

References

1. A. van den Berg, W. Olthuis, and P. Bergveld, "Micro Total Analysis Systems 2000", **2000**, Kluwer Academic Publishers, Dordrecht.
 2. D. Figeys and D. Pinto, *Anal. Chem.*, **2000**, *72*, 330A.
 3. K. Sato, M. Tokeshi, T. Kitamori, and T. Sawada, *Anal. Sci.*, **1999**, *15*, 641.
 4. H. M. Sorouraddin, A. Hibara, M. A. Proskrunin, and T. Kitamori, *Anal. Sci.*, **2000**, *16*, 1033.
 5. M. Tokeshi, T. Minagawa, and T. Kitamori, *Anal. Chem.*, **2000**, *72*, 1711.
 6. M. Tokeshi, T. Minagawa, and T. Kitamori, *J. Chromatogr. A*, **2000**, *894*, 19.
 7. K. Sato, M. Tokeshi, T. Odake, H. Kimura, T. Ooi, M. Nakao, and T. Kitamori, *Anal. Chem.*, **2000**, *72*, 1144.
 8. H. Hisamoto, T. Saito, and T. Kitamori, submitted.
 9. Y. Tanaka, M. N. Slyadnev, A. Hibara, M. Tokeshi, and T. Kitamori, *J. Chromatogr. A.*, **2000**, *894*, 45.
 10. A. E. Kamholz, B. H. Weigl, B. A. Finleyson, and P. Yager, *Anal. Chem.*, **1999**, *71*, 5340.
 11. J. P. Brody and P. Yager, *Sens. Actuators A*, **1997**, *58*, 13.
 12. H.-B. Kim, K. Ueno, M. Chiba, O. Kogi, and N. Kitamura, *Anal. Sci.*, **2000**, *72*, 871.
 13. R. A. Bartsh and J. D. Way, "Chemical Separation with Liquid Membranes: ACS Symposium Series", **1996**, American Chemical Society, Washington, D.C.
 14. M. Harada, K. Iwamoto, T. Kitamori, and T. Sawada, *Anal. Chem.*, **1993**, *65*, 2938.
 15. K. Uchiyama, A. Hibara, H. Kimura, T. Sawada, and T. Kitamori, *Jpn. J. Appl. Phys.*, **2000**, *39*, 5316.
 16. H. Nagatani and H. Watarai, *Anal. Chem.*, **1998**, *70*, 2860.
-